

A Deep Learning Approach to Localizing Multi-level Airway Collapse Based on Snoring Sounds

Ying-Chieh Hsu^{1,2,3}, Stanley Yung-Chuan Liu⁴, Chao-Jung Huang^{4,5}, Chi-Wei Wu⁶, Ren-Kai Cheng⁶, Jane Yung-Jen Hsu⁶, Shang-Ran Huang⁷, Yuan-Ren Cheng⁷, Fu-Shun Hsu^{7,8,9}

¹Department of Biomedical Engineering, National Taiwan University, Taipei, Taiwan.

²Department of Otolaryngology Head and Neck Surgery, Taipei Tzu Chi Hospital, Buddhist Tzu Chi Medical Foundation, Taipei, Taiwan.

³Tzu Chi University, School of Medicine, Hualien, Taiwan.

⁴Division of Sleep Surgery, Department of Otolaryngology, Head and Neck Surgery, Stanford University School of Medicine, Stanford, California, USA.

⁵All Vista Healthcare Center and Center for AI and Advanced Robotics, National Taiwan University, Taipei, Taiwan.

⁶Department of Computer Science and Information Engineering, National Taiwan University, Taipei, Taiwan.

⁷Heroic Faith Medical Science Co., Ltd., New Taipei, Taiwan.

⁸Graduate Institute of Biomedical Electronics and Bioinformatics, National Taiwan University, Taipei, Taiwan.

⁹Department of Critical Care Medicine, Far Eastern Memorial Hospital, New Taipei, Taiwan.

Authors Email Address:

Ying-Chieh Hsu, Department of Biomedical Engineering, National Taiwan University, Taipei, Taiwan. Department of Otolaryngology, Head and Neck Surgery, Taipei Tzu Chi Hospital, Buddhist Tzu Chi Medical Foundation, Taipei, Taiwan. Tzu Chi University, School of Medicine, Hualien, Taiwan. iammed91@gmail.com

Stanley Yung-Chuan Liu, Division of Sleep Surgery, Department of Otolaryngology Head and Neck Surgery, Stanford University School of Medicine, Stanford, California, USA. ycliu@stanford.edu

Chao-Jung Huang, All Vista Healthcare Center and Center for AI and Advanced Robotics, National Taiwan University, Taipei, Taiwan. Department of Otolaryngology Head and Neck Surgery, Stanford University School of Medicine, Stanford, California, USA. cjhuang0717@gmail.com

Chi-Wei Wu, Department of Computer Science and Information Engineering, National Taiwan University, Taipei, Taiwan. aladar.wu@gmail.com

Ren-Kai Cheng, Department of Computer Science and Information Engineering, National Taiwan University, Taipei, Taiwan. b06902127@ntu.edu.tw

Jane Yung-Jen Hsu, Department of Computer Science and Information Engineering, National Taiwan University, Taipei, Taiwan. yjhsu@csie.ntu.edu.tw

Shang-Ran Huang, Heroic Faith Medical Science Co., Ltd., New Taipei, Taiwan. srh623@gmail.com

Yuan-Ren Cheng, Heroic Faith Medical Science Co., Ltd., New Taipei, Taiwan. infie.cheng@heroic-faith.com

Fu-Shun Hsu, Graduate Institute of Biomedical Electronics and Bioinformatics, National Taiwan University, Taipei, Taiwan. Department of Critical Care Medicine, Far Eastern Memorial Hospital, New Taipei, Taiwan. Heroic Faith Medical Science Co., Ltd., New Taipei, Taiwan. fhsu@heroic-faith.com

Abstract

This study investigates the application of machine/deep learning to classify snoring sounds excited at different levels of the upper airway in patients with obstructive sleep apnea (OSA) using data from drug-induced sleep endoscopy (DISE). The snoring sounds of 39 subjects were analyzed and labeled according to the Velum, Oropharynx, Tongue Base, and Epiglottis (VOTE) classification system. The dataset, comprising 5,173 one-second segments, was used to train and test models, including Support Vector Machine (SVM), Bidirectional Long Short-Term Memory (BiLSTM), and ResNet-50. The ResNet-50, a convolutional neural network (CNN), showed the best overall performance in classifying snoring acoustics, particularly in identifying multi-level obstructions. The study emphasizes the potential of integrating snoring acoustics with deep learning to improve the diagnosis and treatment of OSA. However, challenges such as limited sample size, data imbalance, and differences between pharmacologically induced and natural snoring sounds were noted, suggesting further research to enhance model accuracy and generalizability.

Keywords: Drug-induced endoscopy (DISE), obstructive sleep apnea (OSA), snoring acoustics, deep learning, apnea-hypopnea index (AHI), convolutional neural network (CNN).

Introduction

Obstructive sleep apnea (OSA) manifests as recurrent episodes of apnea or hypopnea during sleep. In the United States, OSA affects approximately 13% of men and 6% of women¹. Patients afflicted with OSA commonly present with symptoms such as snoring (often prompting medical consultation), excessive daytime sleepiness, morning headaches, heightened susceptibility to cardiovascular ailments, and increased risk of vehicular accidents. Polysomnography (PSG) is the gold standard for diagnosing OSA, albeit offering limited insights into the precise anatomical locations of upper airway obstruction. A myriad of treatment modalities, both non-invasive and invasive, exist for managing OSA. Non-invasive interventions encompass continuous positive airway pressure (CPAP), oral appliances, weight reduction strategies, and positional therapy^{2,3}, while invasive approaches comprise nasal surgeries, uvulopalatopharyngoplasty, tongue base reduction surgery, genioglossus advancement, and maxillomandibular advancement⁴⁻⁷. However, the efficacy of these treatments varies, necessitating accurate identification of the site of upper-airway obstruction to guide therapeutic decisions. For instance, OSA patients with epiglottic collapse often exhibit poor adherence to CPAP therapy⁸, while oral appliances are more suitable for individuals with tongue base obstruction⁹.

Several invasive techniques exist for localizing upper airway obstructions, including nasofibroscope with the Muller maneuver, upper airway pressure measurement, and drug-induced sleep endoscopy (DISE)¹⁰⁻¹². However, the awake state of patients during the Muller maneuver limits its ability to accurately reflect upper airway dynamics during sleep, leading to substantial discrepancies in identifying sites of collapse compared to DISE, with a reported mismatch rate of 76%¹³. Non-invasive methods for identifying upper airway collapse include computed tomography and dynamic magnetic resonance imaging^{14,15}. Nonetheless, computed tomography poses radiation exposure risks, while dynamic sleep MRI is hindered by excessive noise levels and substantial costs. Among these methods, only DISE enables direct and precise assessment of upper airway collapse during pharmacologically induced sleep^{12,16}.

Acoustic analysis of snoring sounds serves various diagnostic purposes, including OSA diagnosis, localization of upper airway obstruction, and post-operative monitoring¹⁷⁻²⁰. Snoring, the hallmark symptom of OSA, arises from the vibration of collapsed soft tissues during sleep²¹. Notably, the acoustic characteristics of snoring, such as frequency spectrum, exhibit variations corresponding to the locations of soft tissue collapse. Thus, analysis of snoring acoustics offers a promising avenue for pinpointing the precise sites of obstruction, encompassing both single and multi-level obstructions. Notably, multi-level obstructions could present in up to approximately 65% of OSA patients, with single-level obstructions observed in the remaining 35%^{22,23}. However, prior studies investigating obstruction localization through acoustic analysis have primarily focused on identifying single-level obstructions. Given this gap, the current study aims to develop an AI model capable of accurately localizing obstruction sites, including both single and multi-level obstructions, based on snoring sounds in OSA patients. To this end, snoring signals and obstruction site data were concurrently collected during DISE procedures and utilized for training and validating the AI model.

Material and Methods

Subjects

A cohort comprising 39 individuals diagnosed with OSA and aged 20 to 70 years was assembled from outpatient otolaryngology clinics between November 2019 and November 2021. Diagnosis of OSA was corroborated through attended PSG, adhering to the standardized protocols outlined by the American Academy of Sleep Medicine²⁴. Specifically, individuals intolerant to continuous CPAP therapy who actively sought surgical interventions were included in the study. Exclusion criteria encompassed individuals with a history of prior OSA surgery, American Society of Anesthesiologists class 3 or above with a heightened anesthesia risk for a DISE procedure, documented adverse reactions to propofol, or pregnancy status. Before participation, all enrolled subjects provided written informed consent per the guidelines established by the Research Ethics Review Committee of Taipei Tzu-Chi Hospital (permit number: 09-XD-079).

Drug-induced Sleep Endoscopy and Snoring Sound Recording

DISE was conducted within an operating theater under the supervision of a seasoned otolaryngologist for every enrolled subject. Before the procedure, subjects received nasal cavity decongestion and local anesthesia. Sedation was induced through intravenous administration of propofol utilizing a target-controlled infusion system. The subject was kept in a supine position during the procedure. A flexible nasofibroscope was inserted through the subjects' right nostril to evaluate upper airway collapse. The bispectral (BIS) index was maintained between 65 and 70 throughout the DISE procedure to ensure optimal anesthesia depth.

During the DISE procedure, the subjects' breathing sounds were recorded using a digital stethoscope (AccurSound AS-101, Heroic Faith Medical Science Co., Ltd., New Taipei, Taiwan) connected to a smartphone (Mi 9T pro, Xiaomi, Beijing, China). The acoustic patch of the digital stethoscope was securely affixed to the subjects' submental region by tapes. The breathing sounds were sampled at a rate of 4 kHz with a bit depth of 16 bits.

VOTE Labeling on DISE videos

Following the DISE procedure, videos documenting DISE assessments were compiled and subsequently scored using the Velum (V), Oropharynx (O), Tongue Base (T), and Epiglottis (E) categorization system, collectively referred to as the VOTE system. This system delineates anatomical regions, including the soft palate, uvula, lateral pharyngeal wall (V); palatine tonsils, lateral pharyngeal wall (O); tongue base, lingual tonsils (T); and epiglottis (E)²⁵. The endoscopic video snapshots on the left side of Fig 1 a–d display examples of partial upper airway obstruction at the different levels.

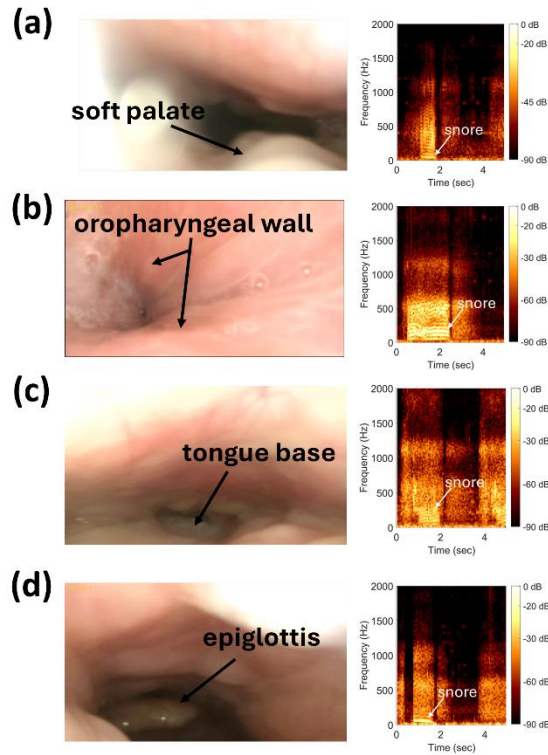


Figure 1. The classification of obstruction sites and their corresponding spectrogram. The endoscopic snapshots on the left side show the obstructions classified at the (a) Velum (V), Oropharynx (O), (c) Tongue Base (T), and (d) Epiglottis (E) levels. The graphs on the right display the temporal-spectral representation of the snoring sounds corresponding to the obstructions. White arrows indicate the features of the snoring sounds.

Segments of DISE videos exhibiting clear visibility were selected for analysis, while those with excessive subject salivation or poor endoscopic views were excluded. These selected DISE segments were independently scored by two experienced otolaryngologists (with sleep surgery fellowship training), and a third otolaryngologist validated their assessments. Given the variability in DISE duration among subjects and the potential for dynamic changes in obstruction locations, only segments deemed acceptable by both experts were included for subsequent model training. Disagreements in VOTE classification between raters led to the exclusion of corresponding DISE segments from the analysis. Following the DISE rating, snoring sounds were categorized as "V," "O," "T," "E," "VO," "VT," "OT," "OE," or "VOT."

VOTE Labeling on Breathing Sounds

The recorded breathing sounds were subsequently transformed into spectrograms using labeling software²⁶, employing a short-time Fourier transform with a Hanning window size of 256 and a hop length of 64. After synchronizing the endoscopic video tapes with the spectrograms, two board-certified otorhinolaryngologists annotated obstruction periods' start and end times according to the video assessment reference. The graphs on the right side of Fig 1 a–d display the spectrogram of snoring sounds excited by the obstructions at the V, O, T, and E levels, respectively.

AI Models for Obstruction Site Classification

We first truncated the labeled periods of the breathing sounds into 1-second segments. The 1-s segments underwent preprocessing to extract various features, serving as the primary input for the AI models. In this study, we trained three different models, namely, bi-directional long short-term memory (BiLSTM) networks²⁷, support vector machine (SVM)²⁸, and ResNet-50 networks²⁹, to classify the 1-s segments based on the obstruction sites.

We distributed the 1-s segments into training and test data sets based on a ratio close to 9:1. In the training data set, one-tenth of the segments were further assigned to the validation set.

For the BiLSTM model, 13 static, 13 delta, and 13 delta-delta Mel-frequency cepstral coefficients (MFCCs)³⁰ were computed, resulting in a total of 39 MFCCs. The MFCCs were calculated with a Hanning window length of 100 and a hop length of 25. An L2 normalizer was used to normalize the MFCCs to a unit form. The normalized MFCCs were fed into the BiLSTM as input.

For the SVM model, we further used the Bag of Audio Words (BoAW) model to encode the MFCCs into new feature vectors^{31,32}. The BoAW model's codebook size was 200, and the assignment was 5.

For the ResNet-50 networks, the Mel-spectrogram was used as model input. The Mel-spectrogram was calculated with a Hanning window length of 2048 and a hop length of 32.

All the feature extraction and model training were completed using Python. The flow chart of feature extraction and model training is displayed in Fig 2.

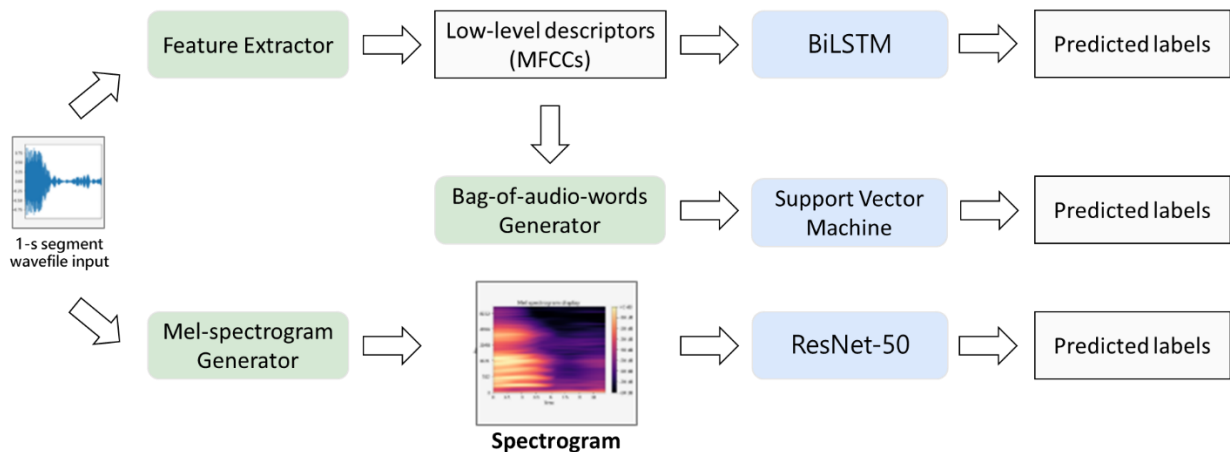


Fig 2. Flowchart of feature extraction and model training. The flowchart illustrates the process of audio signal processing and classification. It begins with an audio waveform input, which is then processed by a feature extractor to obtain low-level descriptors (MFCCs). These MFCCs are then used in two parallel paths: one path involves a Bag-of-audio-words Generator leading to a

Support Vector Machine (SVM), and the other path ultimately goes to a BiLSTM (Bidirectional Long Short-Term Memory) model. The Wave file input also involves a Mel-spectrogram Generator to generate sound spectrogram, leading to a ResNet-50 model to predict labels.

Statistics

Precision, recall, and F1-score are crucial metrics used to evaluate the performance of AI models, especially in classification tasks^{33,34}. These metrics are essential for understanding the performance of AI models, as they provide insights into different aspects of the model's predictive capabilities.

Precision measures the proportion of true positive predictions among all positive predictions made by the model. It indicates how many of the predicted positive instances are positive. High precision means that the model has a low false positive rate. Mathematically, it is defined as:

$$\text{Precision} = \frac{TP}{TP + FP}$$

where TP is the number of true positives and FP is the number of false positives³³.

Recall, also known as sensitivity or true positive rate, measures the proportion of true positive predictions among all actual positive instances. It indicates how well the model can identify positive instances.³⁵ High recall means that the model has a low false negative rate. Mathematically, it is defined as:

$$\text{Recall} = \frac{TP}{TP + FN}$$

The F1-score is the harmonic mean of precision and recall. It provides a single metric that balances both precision and recall, making it useful when you need to consider both false positives and false negatives. Mathematically, it is defined as:

$$\text{F1-score} = 2 \times \frac{\text{Precision} \times \text{Recall}}{\text{Precision} + \text{Recall}}$$

The F1-score is particularly useful in scenarios where the class distribution is imbalanced³⁴.

In this study, we used these three performance indexes to evaluate the trained models.

Results

The average age of the 39 subjects enrolled in this study was 40.05 years. Among them, 33 were male (84%) and six were female (16%). The mean apnea-hypopnea index (AHI) was 39.63 events

per hour. The severity of OSA varied across the cohort, with one subject exhibiting primary snoring (AHI < 5 events/hour), constituting 3% of the total; nine subjects presenting mild OSA (AHI 5–15 events/hour), representing 23% of the total; eight subjects with moderate OSA (AHI 15–30 events/hour), accounting for 20% of the total; and 21 subjects diagnosed with severe OSA (AHI > 30 events/hour), comprising 54% of the total.

The overall duration of the 1-second segment dataset amounted to 5,173 seconds. Specifically, recording numbers for the obstruction sites of the V, O, T, and E totaled 259, 403, 77, and 13 seconds respectively. On the other side, the other snoring records were revealed as mixed VOTE-label, "VO," "VT," "OT," "OE," and "VOT" (Table 1). The train-test ratio was kept equal to 9:1, and the training and test data set sizes were shown in Table 2.

Table 1. 1-s segments distribution of various obstruction levels. The snoring sounds were divided into N, V, O, T, E, VO, VT, OT, OE, and VOT labels, and each recorded snoring sound number was presented with labels.

Label	Number
N	3,150
V	259
O	403
T	77
E	13
VO	1,016
VT	46
OT	140
OE	39
VOT	30
Total	5,173

Table 2. The number of data in the training and test data sets.

	Training	Test
Label	Number	Number
V	902	100
O	714	79
T	205	23
E	54	6
VO	2050	227

VT	210	23
OT	349	38
OE	66	7
VOT	99	11
Total	4696	514

Tables 3, 4, and 5 show the classification performance of the trained models for the SVM, BiLSTM, and ResNet-50 models, respectively.

Table 3. Performance of the SVM model on multi-class classification.

	Precision	Recall	F1-score
V	0.94	0.73	0.82
O	0.80	0.54	0.65
T	0.95	0.83	0.88
E	1.00	0.17	0.29
VO	0.75	0.98	0.85
VT	0.95	0.87	0.91
OT	0.70	0.68	0.69
OE	1.00	0.43	0.60
VOT	0.67	0.18	0.29
Accuracy			0.80
Macro avg	0.86	0.60	0.66
Weighted avg	0.81	0.80	0.78

Table 4. Performance of the BiLSTM model on multi-class classification.

	Precision	Recall	F1-score
V	0.86	0.76	0.81
O	0.63	0.68	0.65
T	0.85	1.00	0.92
E	0.33	0.17	0.22
VO	0.8	0.83	0.82
VT	0.78	0.78	0.78
OT	0.72	0.68	0.7
OE	0.75	0.43	0.55
VOT	0.73	0.73	0.73

Accuracy			0.77
Macro avg	0.72	0.67	0.69
Weighted avg	0.77	0.77	0.77

Table 5. Performance of the ResNet-50 model on multi-class classification.

	Precision	Recall	F1-score
V	0.90	0.82	0.86
O	0.77	0.52	0.62
T	0.72	0.91	0.81
E	0.8	0.67	0.73
VO	0.77	0.89	0.83
VT	0.88	0.65	0.75
OT	0.57	0.66	0.61
OE	1.00	0.86	0.92
VOT	0.83	0.45	0.59
Accuracy			0.78
Macro avg	0.81	0.71	0.75
Weighted avg	0.79	0.78	0.78

Discussion

Earlier studies on the correlation between snoring sounds and upper airway collapse commonly differentiate between palatal and non-palatal snoring. For example, Osborne et al. demonstrated a significantly higher peak factor ratio for palatal snoring compared to non-palatal snoring³⁶. Recent advancements in snore sound classification have focused on labeling snore sounds based on DISE videos. Qian et al. utilized enhanced wavelet features combined with the BoAWs technique for snore sound classification, achieving a 69.4% unweighted average recall (UAR)^{37,38}. Demir et al. explored the use of low-level image texture features in snore sound classification, attaining a 72.6% UAR³⁹. These studies suggest that varying levels of upper airway obstruction manifest in distinct snore sounds, which can be identified using artificial intelligence.

The most prominent snore sound classifier to date has been developed using the Munich Passau Snore Sound Corpus (MPSSC)⁴⁰. Introduced at the INTERSPEECH 2017 Computational Paralinguistic Challenge, the MPSSC dataset encompasses snoring sounds from patients undergoing DISE, collected by three medical centers and classified into four classes. However, this dataset primarily contains single-level obstructions, whereas multi-level obstructions are more prevalent in patients with OSA. Notably, Traxdorf et al.⁴¹ observed a combination of velum and/or oropharyngeal obstructions in 40% of severe OSA patients. While many AI studies analyzing snoring sounds in OSA patients utilize the MPSSC dataset, which predominantly features single-

level obstructions, clinical settings reveal that most patients exhibit multi-level obstructions. To address this discrepancy, we developed models capable of classifying snores associated with multi-level obstructions, thereby aiding physicians in accurately identifying obstruction locations.

Our results revealed the performance of the SVM model on multi-class classification. The model achieved an overall accuracy of 0.80, with macro averages for precision, recall, and F1-score of 0.86, 0.60, and 0.66, respectively. The weighted averages for precision, recall, and F1-score were 0.81, 0.80, and 0.78, respectively. The model performed best on label VT with an F1-score of 0.91 and worst on label E with an F1-score of 0.29. Similarly, the BiLSTM model achieved an overall accuracy of 0.77, with macro averages for precision, recall, and F1-score of 0.72, 0.67, and 0.69, respectively. The weighted averages for precision, recall, and F1-score were all 0.77. The model performed best on label T with an F1-score of 0.92 and worst on label E with an F1-score of 0.22. The ResNet-50 model achieved an overall accuracy of 0.78, with macro averages for precision, recall, and F1-score of 0.81, 0.71, and 0.75, respectively. The weighted averages for precision, recall, and F1-score were all 0.78. The model performed best on label OE with an F1-score of 0.92 and worst on label OT with an F1-score of 0.61. Among the three models, the SVM model demonstrated the highest macro average precision, while the ResNet-50 model had the highest macro average recall and F1-score. The BiLSTM model had the lowest overall performance in terms of accuracy and F1-score. Each model had varying strengths and weaknesses across different labels, indicating that the choice of model may depend on the specific requirements and priorities of the classification task.

The performance of the three models—SVM, BiLSTM, and ResNet-50—on multi-class classification tasks highlights distinct strengths and weaknesses. The SVM model demonstrated the highest macro average precision, indicating its ability to identify positive instances across different classes correctly. However, its recall and F1-score were lower, suggesting it might miss some positive instances. The BiLSTM model, while having the lowest overall accuracy and F1-score, showed strong performance on label T, achieving the highest F1-score among the models. This indicates that BiLSTM might be particularly effective for certain classes, but its overall performance is less consistent. The ResNet-50 model achieved the highest macro average recall and F1-score, indicating a balanced performance in identifying positive instances and minimizing false negatives. Its performance on label V was particularly strong, making it a reliable choice for tasks where this label is critical. In conclusion, the choice of model should be guided by the specific requirements of the classification task. If precision is paramount, the SVM model might be preferred. For tasks requiring high recall and balanced performance, the ResNet-50 model is a strong candidate. The BiLSTM model, despite its lower overall performance, could be valuable for specific classes where it excels. Further fine-tuning and hybrid approaches might also be explored to leverage the strengths of each model.

Given that snoring originates from the vibration of collapsed soft tissues during sleep, we hypothesized that different obstruction levels correspond to distinct audio features. Consequently, mixed-type obstructions may exhibit characteristics of their constituent classes. For instance, "VO" snoring sounds might share audio characteristics of both the velum and oropharynx, potentially leading to misclassification by a deep learning model as "V" or "O" snores. To address this, we devised a snoring sound classification model incorporating single and multi-level obstructions.

This study has limitations. The acoustic features of snoring sounds obtained during DISE may not fully replicate those produced during natural sleep. First, the airway collapse induced by sedation may differ from the collapse during sleep. Induced snoring sounds tend to have a higher frequency component than natural snoring patterns⁴². Propofol sedation also reduces the occurrence of palatal flutter, a significant contributor to snoring sounds⁴³. Second, the endoscope used in DISE might prevent airway collapse or alter the acoustic patterns of vibrating tissues. Third, the subject was supine during DISE, whereas head and body positions may change during natural sleep. Furthermore, we did not differentiate between types of obstruction, such as anterior-posterior, lateral, or concentric velum collapses, nor did we consider the extent of the obstruction. Severe obstructions may not produce any snoring sounds. Additionally, the study encountered challenges related to limited sample size and unbalanced data distribution, which may have compromised the accuracy of the snoring sound classification models. The small dataset and data imbalance made generalizing the snoring sound generation difficult, given the many phenotypes and influential factors involved.

Future research should prioritize expanding the snoring sound dataset to improve model accuracy. Furthermore, investigating the correlation between pharmacologically induced and naturally occurring snoring sounds will be essential. If similarities exist between these two types of snoring sounds, our model may have potential applications in PSG examinations.

Conclusion

In this investigation, we have introduced a novel snoring sound classifier, offering a non-invasive approach to healthcare professionals' precise determination of upper-airway collapse conditions, thereby facilitating tailored treatment strategies. To the best of our knowledge, this study represents a pioneering effort in employing machine/deep learning methodologies to classify snoring sounds associated with single and multi-level obstructions. Our proposed model has impressive overall accuracy with F1-scores between 77–80%. Our findings suggest that these models hold promise as a non-invasive tool for accurately assessing upper-airway conditions.

Acknowledgments: This study received funding from the Taipei Tzu Chi Hospital, Buddhist Tzu Chi Medical Foundation (Grant No. TCRD-TPE-110-16). Additionally, partial support for this research was provided by the All-Vista Healthcare Center and the Center for AI and Advanced Robotics at National Taiwan University, as well as the National Science and Technology Council in Taiwan (Grant No. NSTC110-2634-F-002-049-).

Reference

- 1 Peppard, P. E. *et al.* Increased prevalence of sleep-disordered breathing in adults. *Am J Epidemiol* **177**, 1006-1014, doi:10.1093/aje/kws342 (2013).
- 2 Mohamed, A. M. *et al.* Oral appliance therapy vs. positional therapy for managing positional obstructive sleep apnea; a systematic review and meta-analysis of randomized control trials. *BMC Oral Health* **24**, 666, doi:10.1186/s12903-024-04277-8 (2024).
- 3 Garg, K. *et al.* Positional Obstructive Sleep Apnoea. *Indian J Chest Dis Allied Sci*, doi:10.5005/ijcdas-63-2-89 (2021).
- 4 Holty, J. E. & Guilleminault, C. Maxillomandibular advancement for the treatment of obstructive sleep apnea: a systematic review and meta-analysis. *Sleep Med Rev* **14**, 287-297, doi:10.1016/j.smrv.2009.11.003 (2010).
- 5 Trindade, P. A. K., Nogueira, V. & Weber, S. A. T. Is maxillomandibular advancement an effective treatment for obstructive sleep apnea? Systematic literature review and meta-analysis. *Braz J Otorhinolaryngol* **89**, 503-510, doi:10.1016/j.bjorl.2023.02.007 (2023).
- 6 Zaghi, S. *et al.* Maxillomandibular Advancement for Treatment of Obstructive Sleep Apnea: A Meta-analysis. *JAMA Otolaryngol Head Neck Surg* **142**, 58-66, doi:10.1001/jamaoto.2015.2678 (2016).
- 7 Zhou, N. *et al.* Maxillomandibular advancement versus multilevel surgery for treatment of obstructive sleep apnea: A systematic review and meta-analysis. *Sleep Med Rev* **57**, 101471, doi:10.1016/j.smrv.2021.101471 (2021).
- 8 Andersen, A. P., Alving, J., Lildholdt, T. & Wulff, C. H. Obstructive sleep apnea initiated by a lax epiglottis. A contraindication for continuous positive airway pressure. *Chest* **91**, 621-623, doi:10.1378/chest.91.4.621 (1987).
- 9 Op de Beeck, S. *et al.* Phenotypic Labelling Using Drug-Induced Sleep Endoscopy Improves Patient Selection for Mandibular Advancement Device Outcome: A Prospective Study. *J Clin Sleep Med* **15**, 1089-1099, doi:10.5664/jcsm.7796 (2019).
- 10 Katsantonis, G. P., Maas, C. S. & Walsh, J. K. The predictive efficacy of the Muller maneuver in uvulopalatopharyngoplasty. *Laryngoscope* **99**, 677-680 (1989).
- 11 Katsantonis, G. P., Moss, K., Miyazaki, S. & Walsh, J. Determining the site of airway collapse in obstructive sleep apnea with airway pressure monitoring. *Laryngoscope* **103**, 1126-1131, doi:10.1288/00005537-199310000-00009 (1993).
- 12 Centers for Disease, C. & Prevention. Perceived insufficient rest or sleep among adults - United States, 2008. *MMWR Morb Mortal Wkly Rep* **58**, 1175-1179 (2009).
- 13 Campanini, A. *et al.* Awake versus sleep endoscopy: personal experience in 250 OSAHS patients. *Acta Otorhinolaryngol Ital* **30**, 73-77 (2010).
- 14 Kumar, A. & Dogra, S. Neuropathology and therapeutic management of Alzheimer's disease - An update. *Drugs of the Future* **33**, doi:10.1358/dof.2008.033.05.1192677 (2008).
- 15 Huon, L. K. *et al.* Dynamic upper airway collapse observed from sleep MRI: BMI-matched severe and mild OSA patients. *Eur Arch Otorhinolaryngol* **273**, 4021-4026, doi:10.1007/s00405-016-4131-1 (2016).
- 16 Faestel, P. M., Littell, C. T., Vitiello, M. V., Forsberg, C. W. & Littman, A. J. Perceived insufficient rest or sleep among veterans: Behavioral Risk Factor Surveillance System 2009. *J Clin Sleep Med* **9**, 577-584, doi:10.5664/jcsm.2754 (2013).
- 17 Won, T. B. *et al.* Acoustic characteristics of snoring according to obstruction site

- determined by sleep videofluoroscopy. *Acta Otolaryngol* **132 Suppl 1**, S13-20, doi:10.3109/00016489.2012.660733 (2012).
- 18 Azarbarzin, A. & Moussavi, Z. Snoring sounds variability as a signature of obstructive sleep apnea. *Med Eng Phys* **35**, 479-485, doi:10.1016/j.medengphy.2012.06.013 (2013).
- 19 Karunajeewa, A. S., Abeyratne, U. R. & Hukins, C. Multi-feature snore sound analysis in obstructive sleep apnea-hypopnea syndrome. *Physiol Meas* **32**, 83-97, doi:10.1088/0967-3334/32/1/006 (2011).
- 20 Li, H. Y. *et al.* Changes of snoring sound after relocation pharyngoplasty for obstructive sleep apnoea: the surgery reduces mean intensity in snoring which correlates well with apnoea-hypopnoea index. *Clin Otolaryngol* **40**, 98-105, doi:10.1111/coa.12325 (2015).
- 21 Quinn, S. J., Daly, N. & Ellis, P. D. Observation of the mechanism of snoring using sleep nasendoscopy. *Clin Otolaryngol Allied Sci* **20**, 360-364, doi:10.1111/j.1365-2273.1995.tb00061.x (1995).
- 22 Hessel, N. S. & de Vries, N. Diagnostic work-up of socially unacceptable snoring. II. Sleep endoscopy. *Eur Arch Otorhinolaryngol* **259**, 158-161, doi:10.1007/s00405-001-0428-8 (2002).
- 23 Hessel, N. S., Laman, M., van Ammers, V. C., van Duijn, H. & de Vries, N. Diagnostic work-up of socially unacceptable snoring. I. History or sleep registration. *Eur Arch Otorhinolaryngol* **259**, 154-157, doi:10.1007/s00405-001-0427-9 (2002).
- 24 Berry, R. B. *et al.* Rules for scoring respiratory events in sleep: update of the 2007 AASM Manual for the Scoring of Sleep and Associated Events. Deliberations of the Sleep Apnea Definitions Task Force of the American Academy of Sleep Medicine. *J Clin Sleep Med* **8**, 597-619, doi:10.5664/jcsm.2172 (2012).
- 25 Kezirian, E. J., Hohenhorst, W. & de Vries, N. Drug-induced sleep endoscopy: the VOTE classification. *Eur Arch Otorhinolaryngol* **268**, 1233-1236, doi:10.1007/s00405-011-1633-8 (2011).
- 26 Fu-Shun Hsu, C.-J. H., Chen-Yi Kuo, Shang-Ran Huang, Yuan-Ren Cheng, Jia-Horng Wang, Yi-Lin Wu, Tzu-Ling Tzeng, Feipei Lai. Development of a Respiratory Sound Labeling Software for Training a Deep Learning-Based Respiratory Sound Analysis Model. doi:10.48550/arXiv.2101.01352 (2021).
- 27 Ibomoiye Domor Mienye, Theo G. Swart & Obaido, G. Recurrent Neural Networks: A Comprehensive Review of Architectures, Variants, and Applications. doi:10.3390/info15090517 (2024).
- 28 Awad, M. & Khanna, R. in *Efficient Learning Machines: Theories, Concepts, and Applications for Engineers and System Designers* 39-66 (Apress, 2015).
- 29 Harini, M. *et al.* 255-265 (Springer Nature Singapore).
- 30 Sueur, J. 381-398 (Springer International Publishing, 2018).
- 31 Vetráb, M. & Gosztolya, G. 285-293 (Springer International Publishing).
- 32 Schmitt, M. & Schuller, B. W. openXBOW Introducing the Passau Open-Source Crossmodal Bag-of-Words Toolki. doi:10.48550/arXiv.1605.06778 (2016).
- 33 Yacouby, R. & Axman, D. (Association for Computational Linguistics).
- 34 Naidu, G., Zuva, T. & Sibanda, E. M. 15-25 (Springer International Publishing).
- 35 Hand, D. J., Christen, P. & Kirielle, N. F*: an interpretable transformation of the F-measure. *Mach Learn* **110**, 451-456, doi:10.1007/s10994-021-05964-1 (2021).
- 36 Osborne, J. E., Osman, E. Z., Hill, P. D., Lee, B. V. & Sparkes, C. A new acoustic method of differentiating palatal from non-palatal snoring. *Clin Otolaryngol Allied Sci* **24**, 130-

- 133, doi:10.1046/j.1365-2273.1999.00229.x (1999).
- 37 Nunez-Batalla, F. *et al.* [Adaptation and validation to the Spanish of the Voice Handicap Index (VHI-30) and its shortened version (VHI-10)]. *Acta Otorrinolaringol Esp* **58**, 386-392 (2007).
- 38 Qian, K. *et al.* A Bag of Wavelet Features for Snore Sound Classification. *Ann Biomed Eng* **47**, 1000-1011, doi:10.1007/s10439-019-02217-0 (2019).
- 39 Demir, F., Sengur, A., Cummins, N., Amiriparian, S. & Schuller, B. Low Level Texture Features for Snore Sound Discrimination. *Annu Int Conf IEEE Eng Med Biol Soc* **2018**, 413-416, doi:10.1109/EMBC.2018.8512459 (2018).
- 40 Janott, C. *et al.* Snoring classified: The Munich-Passau Snore Sound Corpus. *Comput Biol Med* **94**, 106-118, doi:10.1016/j.compbiomed.2018.01.007 (2018).
- 41 Traxdorf, M. *et al.* Drug-induced sleep endoscopy (DISE) with target controlled infusion (TCI) and bispectral analysis in obstructive sleep apnea. *JoVE (Journal of Visualized Experiments)*, e54739 (2016).
- 42 Agrawal, S., Stone, P., McGuinness, K., Morris, J. & Camilleri, A. E. Sound frequency analysis and the site of snoring in natural and induced sleep. *Clin Otolaryngol Allied Sci* **27**, 162-166, doi:10.1046/j.1365-2273.2002.00554.x (2002).
- 43 Jones, T. M., Ho, M. S., Earis, J. E., Swift, A. C. & Charters, P. Acoustic parameters of snoring sound to compare natural snores with snores during 'steady-state' propofol sedation. *Clin Otolaryngol* **31**, 46-52, doi:10.1111/j.1749-4486.2006.01136.x (2006).